Origin of the Harappan Ernestites: Fabrication and Raw Materials

M.K. Mahala[1], Jyotiranjan S. Ray[1,*], A.K. Kanungo[2], G.N.S. Sree Bhuvan[3], A. Chatterjee[1,4], B.G. George[5], N. Sorcar[6,7], Y.S. Rawat[8], J.S. Kharakwal[9], and S.V. Rajesh[10]

[1]Physical Research Laboratory, Navrangpura, Ahmedabad 380009, India
[2]Indian Institute of Technology Gandhinagar, Palaj, Gandhinagar 382055, India
[3]Department of Earth Sciences, Pondicherry University, Puducherry 605014, India
[4]Department of Geology, Presidency University, College Street, Kolkata 700073, India
[5]Department of Earth Sciences, Indian Institute of Technology Bombay, Mumbai 400076, India
[6]National Centre for Earth Science Studies, Akkulam, Thiruvananthapuram 695011, India
[7]Korea Polar Research Institute, Incheon 21990, Republic of Korea
[8]Archaeological Survey of India, Dharohar Bhawan, 24 Tilak Marg, New Delhi 110011, India
[9]JRN Rajasthan Vidyapeeth, Sahitya Sansthan, Udaipur 313001, India
[10]Department of Archaeology, University of Kerala, Thiruvananthapuram 695581, India

*Correspondence: jsray@prl.res.in

Abstract

Significant developments in stone bead technology in South Asia, including drilling techniques, happened during the Harappan civilization. Among the stone drill bits used for bead making, long and constricted cylindrical drill bits made from a unique stone named Ernestite were exclusive to the Harappan civilization. Most Ernestites have been discovered in the Harappan cities in Gujarat, India. The origin of Ernestite remains a mystery without a natural analog and unknown manufacturing process. Here, we present the results of a detailed textural, mineralogical, geochemical, and Sr-Nd isotopic investigation of Ernestite stones and drill bits from three Harappan sites and one Sorath Harappan site in Gujarat carried out to understand their manufacturing process and establish the provenance of the raw materials used. $^{87}Sr/^{86}Sr$ and $\varepsilon_{Nd}(0)$ genetically link the drill bits to the Ernestite stones. The texture, pseudomullite (aluminosilicate with SiO_2 > 40 wt%) matrix, and high substitutions of Al_2O_3 (> 10 wt%) and TiO_2 (> 30 wt%) in hematites point to Ernestites' synthetic origin via a sintering process, with the temperature reaching ~1100°C. The abundant sand-to-silt-sized detrital quartz and detrital hematite, ilmenite, rutile, and zircon suggest that the Harappans used crudely powdered sandstones and laterites as raw materials. The major oxide contents (SiO_2 > 40 wt%; Al_2O_3 > 20 wt%; TiO_2 > 1 wt%), Primitive Mantle-normalized trace element patterns, and Sr-Nd isotopic compositions ($^{87}Sr/^{86}Sr$ < 0.731 and $\varepsilon_{Nd}(0)$ > -18.3) of the Ernstite whole-rocks not only support sand-laterite mixtures as basic ingredients but hint at a regional provenance for the raw materials, within the Kutch region of Gujarat.

Keywords: Bronze Age, Harappan Civilization, Ernestite, cylindrical drill bits, Dholavira, Bhagatrav, Kanmer, Khirsara

1. Introduction

Stone beads are one of the critical indicators of cultural and trade practices within prehistoric South Asian civilizations (Kenoyer, 2017a; Kenoyer and Vidale, 1992). Manufacture of stone beads began with the perforation of soft stones (e.g., limestone, steatite, lapis lazuli) and later with hard stones (e.g., chert, agate, and jasper). The earliest evidence of stone beads dates

back to the Mesolithic period (Jwalapuram; Clarkson et al., 2008); significant developments in bead production technologies, such as drilling, shaping, coloring, and mounting onto ornaments, occurred in the Neolithic and Chalcolithic periods (Kenoyer, 2017a) and became a key component of regional and external trades during the Indus valley (Harappan) civilization (Kenoyer, 2007, 2017a,b; Law, 2011). Although various beads of different materials were in use, the long cylindrical beads of harder stones, typically jasper and carnelian, were manufactured through perforation using constricted cylindrical drill bits cut out from unique chips/stones (Kenoyer and Vidale, 1992; Kenoyer, 2003, 2005; Prabhakar et al., 2012). Kenoyer and Vidale (1992) temporarily named these stones "Ernestite" (after Ernst J.H. Mackay). This name is still in use. The constricted cylindrical drill bits have a long cylindrical shape that is typically wide at the tip and narrow at the mid-section (Fig. 2b), resulting in a drill hole section with a stepped profile (Kenoyer, 2017a). The Ernestite drill bits were primarily manufactured by the artisans of the Harappan civilization (Kenoyer, 2017b; Kenoyer et al., 2022). Ernestite drill bits became almost extinct in subsequent cultural periods (Kenoyer, 2015; Ludvik et al., 2022).

Despite their ubiquitous presence in the Harappan settlements (Fig. 1), the origin of the Ernestite stones and drill bits remains uncertain. Kenoyer and Vidale (1992) speculated that these stones are of metamorphic origin. Later, Law (2011), based on his limited mineralogical/chemical data and data from earlier experimental studies on clays, speculated that the Ernestite was a transformed claystone produced by heat treatment (~1100 °C) to achieve the desired hardness. Although Law (2011) tried to justify the presence of the constituent minerals, he did not establish if all of these were produced during the heating process or if some could have been detrital. Besides, he did not explain why the so-called mullites in the Ernestites contained much less Al_2O_3 and higher SiO_2 than stoichiometry mandated (e.g., Shears and Archibald, 1954). Similarly, ambiguity persists about the provenance (source regions) of the Ernestite raw materials as earlier workers (Law, 2011; Prabhakar et al., 2012) proposed both local (Kutch/Ratanpur) and regional (Gujarat) sources, and there exists no isotopic data to establish the source(s) conclusively.

Deciphering Ernestite source materials and their geologic origin are vital to understanding the stone drilling technology and the inter-regional communication network during the Harappan period. In this study, we have addressed the following poorly understood aspects of the Ernestites with detailed petrography, mineralogy, mineral chemistry, geochemical and isotopic investigations from three Harappan sites (Dholavira, Khirsara, Kanmer) and one Sorath Harappan site (Bhagatrav) in Gujarat, India: (1) What is the nature of Ernestites, (2) If artificial, what raw materials were used for their manufacturing, and (3) What were the geologic sources for these raw materials? In addition, we have attempted to shed some light on the manufacturing process of these stones.

2. Background and Previous Work

Ancient Gujarat was well known for its rich agate resources, which attracted the Harappans to this region, and bead manufacturing industries/workshops were established in several urban centers in Kutch and Saurashtra (Law, 2011, 2013). It is generally believed that the Ernestite drill bits were primarily used for making long cylindrical carnelian beads since their hardness is higher than agate (~7.5 on Mohs' scale; Kenoyer, 2017b; Law, 2013; Prabhakar, 2016). The Ernestite is a signature finding of the urban phase of the Harappan civilization; however, they have been reported in large numbers from the late phase, single-cultured Harappan and Sorath Harappan sites as well (Prasad and Prabhakar 2022, Nath and Kumaran

2017; Pokharia et al. 2017). Some important Harappan and Sorath Harappan sites, including those where Ernesites have been reported, are shown in the map (Fig.1). Many Ernestite stones and drill bits have been found in close association with bead workshops in several Harappan sites in Pakistan (e.g., Harappa, Mahenjo-daro, Chahnudaro; Mackay, 1937, 1938; Kenoyer & Vidale, 1992; Law, 2011) as well as in India (e.g., Dholavira, Khirsara, Kanmer, Bisht, 2015; Prabhakar et al., 2012; Nath & Kumaran, 2017; Pokharia et al., 2017; Kharakwal et al., 2008, 2012), and in a few Sorath Harappan sites such as Bhagatrav, Bagasra, Shikarpur, Nagwada (Chase et al., 2014; Bhan, 2018; Prasad & Prabhakar, 2022; and references therein).

Kenoyer and Vidale (1992) described Ernestite at Mohenjo-daro as a rock composed of a mottled greyish-green to yellow-brown matrix with dark brown to black irregular patches or dendritic formations, and based on the XRD analysis of samples from Mohenjo-daro, Chanhudaro, and Harappa, they opined that these are metamorphic rocks composed of quartz, sillimanite, mullite, hematite, and titanium oxide phases. Law (2011) observed significant quartz, mullite-sillimanite, and hematite phases in two samples from Harappa and mullite and cristobalite in the other two. He found from XRD and EMPA analyses that the light and dark matrices consisted of clay-sized (< 2 μm) Al-Si bearing phases, compositionally similar to mullite and sillimanite, apart from quartz. The dark matrix contained additional phases such as hematite, titanohematite, rutile, and zircon. Law (2011) suggested that the Ernestite is likely a highly indurated tonstein flint clay, sufficiently heat treated to yield Ernestite characteristics. However, no experimental proof was provided for transforming any natural rock or mineral to Ernestites by heating.

Tonstein is a kaolinitic (flint) clay stone formed by diagenesis of volcanic ash in a swampy or non-marine environment (Spears 2012). Despite a detailed analysis of Ernestites, Law (2011) did not provide the locations of the probable sources of tonstein. Because of the sheer number of Ernestite drill bits reported from the Harappan city of Dholavira in Gujarat (1212), Prabhakar et al. (2012) hypothesized that the sources of Ernestite raw materials were located within the Kutch province of Gujarat. The XRD analyses of two samples of Ernestites from Dholavira and one sample from Bhgatrav, done by Prabhakar et al. (2012) and Prasad and Prabhakar (2022), respectively, showed the presence of quartz, hematite, and sillimanite/mullite. No cristobalite has been reported in Ernestites from any of the Indian sites.

3. Materials and Methods

Owing to our limited access to the Harappan artifacts, only six samples could be included in this study consisting of three Ernestite stone/rock samples (Fig. 2a) and three drill bits (Fig. 2b) from four sites (Khirsara, Kanmer, Dholavira, and Bhagatrav; Fig. 1) in Gujarat. The sample from Kanmer is associated with the mature Harappan phase and comes from the collection of Kharakawal et al. (2012). The Bhagatrav sample is related to the Sorath Harappan phase (Kanungo et al., 2025) and comes from the collection of Kanungo (2021). Sample from Dholavira represents the Mature/Late Harappan phase (Bisht, 2015). The stratigraphic contexts of the samples can be found in the references given for each location. The Ernestite from Bhagatrav was subsampled into three; there were two drill bits from Kanmer (the first and third from the left in Fig. 2b) and one from Khirsara. Two laterite samples and two sandstone samples from the island of Khadir, on which Dholavira is located, were also studied. Because of their size and rarity, the drill bits were analyzed only for Sr-Nd isotopic compositions, whereas the stones/rocks were powdered for mineralogical, geochemical, and isotopic analyses.

Petrographic studies were conducted on thin sections of all three Ernestite samples using transmitted and reflected lights. Grain size analysis was done using the inbuilt software (Stream Basic) associated with the petrographic microscope (Olympus® BX-53). The mineralogical compositions of the Dholavira and Bhagatrav Ernestites whole rock powders were determined by X-ray diffraction (XRD) using a Bruker D2 Phaser diffractometer at the Physical Research Laboratory (PRL). The major element contents of Ernestites were determined by X-ray Fluorescence (XRF) spectroscopy using a Rigaku® Supermini200 instrument at PRL and the pressed pellet method (Tripati et al., 2022). Multiple international rock standards were used for calibration, and the reference material OU-6 from the International Association of Geoanalysts (IAG) was used for accuracy and precision checks. The major element contents of laterites and sandstones were measured at the National Centre for Earth Science Studies (NCESS), Thiruvananthapuram, using an S4 Pioneer sequential wavelength dispersive-XRF, with reference materials VL-1 and MAG-1 used for accuracy and precision checks (Table S1; Kumar and Sreejith, 2016). In-situ mineral chemical analyses were conducted using a CAMECA SX-5 Tactics Electron Probe Microanalyzer (EPMA) at NCESS (Dev et al., 2022; Sorcar et al., 2021). Analyses were performed at 20 kV accelerating voltage and 20 nA beam current with a beam diameter of 1μm.

Bulk sample geochemical and isotopic measurements were carried out at PRL. About 50 mg of sample powder each was digested using conventional HF-HNO_3 and HF-HNO_3-HCl dissolution protocols for trace element and isotopic analyses, respectively. The details of the analytical procedures are given in George and Ray (2017). Trace element concentrations were measured on a Thermo® HR-ICPMS using BHVO-2 (USGS) as a calibration standard. Machine drift correction was performed using ^{115}In as an internal standard. The accuracy and precision of our measurements, determined by repeated analyses of BHVO-2 (as unknown), were better than 2% for REE and 5% for other trace elements. Sr and REE were separated from digested solutions by conventional cation exchange column chromatography using AG 50W-X8 resin (BioRad®), and Nd was eluted from REE using Ln-specific resin (Eichrom®), using protocols given in George and Ray (2017). Sr and Nd isotopic ratio measurements were performed on a TIMS (Thermo® Triton Plus) in static multicollection mode. Sr isotopes of some samples were measured on an MC-ICPMS at PRL (Chatterjee and Ray, 2018). Instrumental mass fractionation for Sr and Nd isotopic ratios was corrected using exponential fractionation (internal) correction equations of Thirlwall (1991) and assuming $^{88}Sr/^{86}Sr$ = 8.375209 and $^{146}Nd/^{144}Nd$ = 0.7219. Multiple measurements of SRM-987 and JNdi-1 over three years yielded an average of $^{87}Sr/^{86}Sr$ = 0.710249±0.000009 (2σ; n = 14) and $^{143}Nd/^{144}Nd$ = 0.512102±0.000010 (2σ; n = 14).

4. Results

4.1 Petrography and Mineralogy

All Ernestite stone chips from Dholavira, Kanmer, and Bhagatrav are heterogeneous in physical appearance (Fig. 2a). They are hard (harder than quartz), highly compact, do not make streaks, and are difficult to break. Two clear domains, a yellowish-brown or khaki color phase and a black color phase, can be distinguished by the naked eye (Fig. 2b). Transmitted and reflected light microscopy reveals that Ernestite stones contain detrital subangular to subrounded quartz grains (sand to silt-sized) and angular to sub-angular opaque phases like hematite and ilmenite set in a compact, fine-grained, light-colored (yellowish/khaki) groundmass of unidentifiable mineral(s) (Fig. 3). Quartz in Dholavira Ernestite occurs as fractured angular to subangular grains (Fig. 3a,b) compared to the sub-angular to sub-rounded grains in Bhagatrav (Fig. 3c,d) and Kanmer (Fig. 3e,f). The opaque phases (hematite,

titanohematite, and ilmenite) appear as narrow bands or irregular patches. They occur in lower proportions in the Dholavira Ernestite than in the Kanmer and Bhagatrav stones. Hematite appears gray and displays the characteristic reddish internal reflection under plane and cross-polar view, respectively, in reflected light (Fig. 3g,h) and is often associated with ilmenite (shows bi-reflectance). All these detrital phases are essentially larger than clay-sized (~4 μm) mineral grains that constitute a clay stone. Sand-sized (210-736 μm diameter; Supplementary Figure 1) detrital grains of ilmenite and its partial replacement by hematite are also observed in the Kanmer Ernestite under a cross-polar view in reflected light (Fig. 3e,f). Zircon and rutile in Kanmer Ernestite have subrounded to irregular grain boundaries, confirming their detrital nature (Supplementary Figure 3). The size (longest diameter) distributions of detrital quartz grains (measured in the thin sections) in Dholavira, Kanmer, and Bhagatrav Ernestites are presented in a box plot (Fig. 4). Their ϕ (= $-\log_2 d$; d = diameter) sizes (1.84-6.64) vary between medium sand to fine silt, with half of the distributions falling between very-fine sand to coarse silt fractions. The quartz grains in Kanmer and Dholavira stones are moderately sorted (1σ = 0.81 and 0.71, respectively), whereas those in the Bhagatrav stone are moderately well-sorted (1σ = 0.68). Powder XRD patterns of the Dholavira and Bhagatrav samples (Supplementary Figure 2) reveal that quartz is the most abundant phase in all the samples, followed by a mullite-like phase (mullite/sillimanite). Hematite was detected only in the Bhagatrav dark matrix (Supplementary Figure 2), though it is observed in the petrography of all Ernestites.

4.2. Major and Trace elements

The major oxide and trace element contents of two Ernestite samples from Bhagatrav and Dholavira, as well as two laterite and two sandstone samples from Khadir island, are presented in Supplementary Data 1. SiO_2 content (47-61 wt%) is the highest among all oxides, with Al_2O_3, FeO^T, and TiO_2 being other major components. MnO, Na_2O, and P_2O_5 are either very low (< 0.1wt%) or absent, whereas K_2O and MgO concentrations are minor. Bhagatrav Ernestite has lower SiO_2 and Al_2O_3, FeO_T, and TiO_2 than Dholavira Ernestite. The major oxide data of the laterite and sandstone samples from the Khadir island are also presented in Supplementary Data 1. Laterites have high Fe_2O_3 (36.7-37.6 wt%), moderate SiO_2 (32.31-32.61 wt%) and low Al_2O_3 (8.77-8.89 wt%), TiO_2 (1.32-1.34 wt%) contents, whereas sandstones are characterized by high SiO_2 (67.57-68.42 wt%), moderate Al_2O_3 (13.26-13.19), K_2O (1.83-1.84 wt%) and low Fe_2O_3 (2.06-2.09 wt%). Various oxides vs. SiO_2 diagrams plotted for Ernestites, sandstones, and laterites, along with the published data for Mesozoic sandstones (Mandal et al., 2016; Periasamy and Venkateshwarlu, 2017) and laterites-bauxites of Kutch (Meshram and Randive, 2011; Jadhav et al., 2012; Singh and Srivastava, 2019), are presented in Fig. 5. Figure 6 presents the primitive mantle (PM) normalized multi-element patterns for the Ernestite samples and those for Mesozoic rocks (Chaudhuri et al., 2020), and laterites of Kutch region (Singh and Srivastava, 2019).

Mineral Chemistry

Representative backscattered electron (BSE) images of various phases in a polished thin section of the Kanmer Ernestite are given in Supplementary Fig. 3. Mineral compositions of different phases are provided in Supplementary Data 2. X-ray elemental maps for all three Ernestite stones (i.e., Kanmer, Bhagatrav, and Dholavira) and chemical spot analysis (both by EPMA) data are provided in Supplementary Figs. 3-6 and Supplementary Data 2. Quartz (SiO_2: 98-100 wt%) of varying sizes are scattered within the light-colored (yellow) fine matrix, mainly consisting of aluminosilicate phases (SiO_2: 40-53 wt%; Al_2O_3: 40-50 wt%).

Although identified as mullites by XRD, the aluminosilicate matrix phases contain much higher SiO_2 than that mandated by stoichiometry (i.e., < 30 wt%; Lentz et al., 2019), therefore, we identify these phases as pseudomullites. Fe-Ti bearing phases, such as hematite (FeO: 71-74 wt%) and ilmenite (TiO_2: 51-56 wt%), often occur as narrow patches or are finely dispersed within the light (yellow) matrix. Many hematite grains have high TiO_2 content (29-40 wt%), thus can be classified as titanohematite. The titanohematites also contain an appreciable amount of Al_2O_3 (5-21 wt%).

4.3. Sr-Nd isotopic ratios

Results of Sr and Nd isotopic compositions of Ernestite whole rocks and drill bits, laterites, and sandstones are provided in Table 1. The $^{87}Sr/^{86}Sr$ and $\varepsilon_{Nd}(0)$ of Ernestite stones and drill bits from Kutch (Dholavira, Kanmer, and Khirsara) vary between 0.71000 and 0.72282, and -14.7 and -13.9, respectively. In contrast, the Sr-Nd isotopic compositions of Bhagatrav Ernestites are more radiogenic in Sr and less radiogenic in Nd ($^{87}Sr/^{86}Sr$ = 0.73022 to 0.730876; $\varepsilon_{Nd}(0)$ = -18.3 to -18.1). The drill bits from Kanmer have identical $\varepsilon_{Nd}(0)$ of -13.9, and one of the drill bits has almost identical $^{87}Sr/^{86}Sr$ as that of the Ernestite stone (0.72282 vs. 0.72207; Table 4). The laterite samples collected from the Khadir (Dholavira) have $^{87}Sr/^{86}Sr$ varying from 0.7089 to 0.7096, and their $\varepsilon_{Nd}(0)$ ranges from -7.7 to -7.5, whereas the sandstones have more radiogenic Sr and Nd ($^{87}Sr/^{86}Sr$ = 0.71494 and 0.74344; $\varepsilon_{Nd}(0)$ = -23.5 and -17.7).

5. Discussion

5.1. The Making of Ernestites

In the first-ever detailed characterization, Kenoyer and Vidale (1992) suggested a metamorphic origin for Ernestites based on their identification of the matrix phases as sillimanite and mullite. Mullite is a rare mineral and has only been reported from specific contact-metamorphic rocks (in metamorphosed clays) and pseudotachylites (Deer et al., 2013; Moecher and Brearley, 2004). It is also commonly observed in high-temperature ceramics and has been synthesized by high-temperature (> 1100°C) heating of various aluminosilicate minerals (e.g., kaolinite, kyanite, andalusite, sillimanite, etc.; Chin et al., 2017; Komarneni et al., 2005; Septawendar, 2007; Worral, 1968). However, we identify these phases, which show identical XRD spectra as mullite, as pseudomullites based on their higher SiO_2 contents (> 40 wt%). Since mullite and pseudomullite are isostructural, all earlier studies, relying primarily on XRD data, had identified pseudomullite as mulite. "Pseudomullite" refers to a structure or phase that resembles mullite (Fig. 7) but is not the true, stoichiometric mullite. It can be formed by decomposition of kaolinite or other aluminosilicate materials (e.g., Worral, 1968; Querol et al., 1994; Noghani and Emami, 2014). Mullite refers to an experimentally observed solid solution series $Al_{4+2x}Si_{2-2x}O_{10-x}$ with $0.2 < x < 0.9$ (Fig. 7; Lenz et al., 2019; Schneider et al., 2008). According to Shears and Archibald (1954), the stoichiometric composition of synthetic mullite commonly varies between $3Al_2O_3.2SiO_2$ (~72wt% Al_2O_3) and $2Al_2O_3.SiO_2$ (~78wt% Al_2O_3). In natural mullites, Fe_2O_3 substitutes Al_2O_3, producing a wide range of compositions at ~30 wt% SiO_2 (Fig. 7; Moecher and Brearley, 2004; Lenz et al., 2019), whereas stoichiometric sillimanite has ~61 wt% Al_2O_3 (Fig. 7). The aluminosilicate phase in Ernestite matrix are pseudomullites and have higher SiO_2 and lower Al_2O_3 than those of natural mullite or silimanite (Fig.7). Pseudomullites are not found in nature and have been shown in synthetic heating experiments to be developed as an intermediate phase during kaolinite to mullite transformation at high temperature (~1100°C; Worral, 1968; Yanti and Pratiwi, 2018). Therefore, the presence of

pseudomullites unambiguously rules out that Ernestites are natural rocks, indicating their origin by high-temperature processing.

The Harappans artificially produced the Ernestites as the source stones for drill bits through some high-temperature heating process that could generate the pseudomullites. Further evidence for a high-temperature process comes from the chemical composition of Fe-Ti bearing phases as determined by EPMA analyses. The presence of titanohematites with significant TiO_2 (29-40 wt%) and Al_2O_3 (5-21 wt%) suggests an extensive substitution between Fe_2O_3 and TiO_2 and between Fe_2O_3 and Al_2O_3. It is known that at temperatures below 800°C, only a limited solid solution between TiO_2 and Fe_2O_3 is possible (Deer et al., 1992). Similarly, in the Fe_2O_3-Al_2O_3 system, higher Al_2O_3 (up to 10 wt%) can be substituted in the hematite (Fe_2O_3) structure at high temperatures only (~1000°C; Deer et al., 1992). Therefore, higher TiO_2 and Al_2O_3 in the titanohematite confirms a heating process (> 1000°C) in Ernestite manufacturing. It is thus apparent that the pseudomullite matrix was produced during high-temperature sintering. This provides the first geochemical evidence of sintering being utilized in manufacturing Ernestites. This also successfully explains the presence of high-temperature craft objects such as stoneware bangles (Pracchia et al., 1993; Vidale, 2000), steatite beads (Barthelmyde Saizieu and Bouquillon, 1994), and furnaces (Kharakwal et al., 2008, 2012) in the Harappan sites. The presence of detrital quartz grains, ilmenite, hematite, zircon, and rutile suggests that the raw materials used for making the Ernestites are natural, even though the process was artificial.

5.2. Raw Materials and Provenance

Law (2011) suggested tonstein flint (kaolinitic claystone) as the only raw material for Harappan Ernestites. He attributed the coarser (up to 100 μm) subhedral quartz or cristobalite grains (detected in his BSE images) to the recrystallized free silica (released during heating) and zircon to a magmatic origin. He suggested that the raw materials for the Ernsitites (i.e, tonsteins) were sourced from local/regional sources (i.e., Kutch). Tonsteins are hard and compact kaolinite-altered volcanic ash layers, generally found in coals and associated sediments (Spears, 2012). These often contain magmatic quartz and zircon (Lyons et al., 1994; Spears, 2012). However, as we observed (section 4.1), quartz, zircon, ilmenite, and rutile in Ernestites are detrital. Therefore, tonstein flint is ruled out as Ernestite's raw material. Additional evidence against using tonsteins for Ernestites comes from the presence of non-radiogenic Nd in the Ernestites ($\varepsilon_{Nd}(0) < -14$), because all ash beds in Kutch are linked to the Deccan Traps (Singh and Srivastava, 2019), which contain more radiogenic Nd ($\varepsilon_{Nd}(0) > -11$, Fig. 8).

The detrital quartz grains' size and moderately sorted nature suggest using coarser raw materials, such as sandstones, which were likely pounded to sand/silt-sized particles before being processed for sintering. It is possible that the Fe-Ti phases (hematite, titanohematite, ilmenite, rutile) observed in the Ernestites also came from the sandstones since sandstones generally contain such heavy minerals. However, our Ernestites appear to show mixing trends between Mesozoic sandstones and laterites-bauxites of the Kutch region in various oxides vs. SiO_2 plots (Fig. 5). Trace element patterns (Fig. 6) also advocate for such a mixture being necessary to explain the chemistry of the Ernestites. Besides, high contents of Al_2O_3 (> 20 wt%) and high field strength elements (e.g., Sc, V, Cr, and Co) in Ernestites cannot be achieved by the sandstones of the Kutch alone. Therefore, a second end-member, containing Fe-Ti minerals but low in alkali elements, is needed to explain the Ernestite chemistry, and the laterites of Kutch, derived from the mafic volcanic rocks of the Deccan Traps, fit the bill.

The Paleocene to Eocene lateritic deposits in western Kutch (Matanomadh Formation) and Saurashtra (Jamnagar) contain both Al-rich (gibbsite, kaolinite) and Fe-rich (goethite, hematite, ilmenite-rich) phases and are depleted in alkalis (Meshram and Randive, 2011; Jadhav et al., 2012; Singh and Srivastava, 2019) have the required characteristics of this raw material. Although we discard claystone as the sole raw material, we do not deny its possible use in combination with sandstone and laterite for Ernestite manufacturing.

Since kaolinite is a common mineral in laterites, it could have decomposed and undergone subsequent chemical and structural changes to form the pseudomullite matrix during the sintering process. The free (amorphous) silica released during the heating of pure kaolinite recrystallizes as cristobalite upon further heating (to ~1350°C; Worral, 1968) and when kaolinite is heated with alumina-bearing material (e.g., bauxite, aluminum fluoride, aluminum hydroxide), free silica formation is prohibited (Chatterjee and Panti, 1965; Locsei, 1968; Rossini et al., 1970). We suspect that during the sintering process carried out by the Harappans, the free silica (SiO_2) formation was suppressed by the presence of gibbsite ($Al(OH)_3$) in the laterite. Moreover, gibbsite undergoes thermal decomposition to boehmite (AlOOH) at 200°C, which transforms into a transitional alumina (α- Al_2O_3) phase at 500°C (Baranyai et al., 2013; Kloprogge et al., 2002). We suspect that the Al_2O_3 in the titanohematite structure was sourced from gibbsite (lateritic) in the mixture during the α-Al_2O_3 stage. Since the results of our study point to a maximum temperature of 1100°C for the sintering process, the cristobalites observed by Law (2011) likely represent a higher temperature or longer heating process.

Similar $^{87}Sr/^{86}Sr$ and $\varepsilon_{Nd}(0)$ of Ernestite stone and drill bits from Kanmer genetically link drill bits to the stone. Although it has been well established that Ernestite stones are the raw materials for long and constricted cylindrical drill bits (e.g., Law, 2011), their isotopic similarity is the first-ever chemical evidence for the same. Because of the sheer number of Ernestite stones and drill bits from Dholavira, Law (2011) speculated that the raw materials for the stones came from either the island itself (i.e., Khadir) or the Kutch region of Gujarat. However, our geochemical data (Figs. 5 and 6) support a regional sourcing of the raw materials. The sandstones and laterites of Kutch appear to have been the primary sources of the raw materials for the Ernestites. In search of more robust evidence for this geological provenance hypothesis, we make use of the Sr-Nd isotopic compositions of Ernestites and their potential source rocks (Table 1; Fig. 8). Although, the ε_{Nd} and $^{87}Sr/^{86}Sr$ compositions of the Ernestites plot well within the compositional field of the Mesozoic sandstones of Kutch, they can be explained by a two-component mixing between the sandstones and laterites of Khadir (Fig. 8). The isotopic compositions of laterites of Khadir, which are developed over volcanic ash of Deccan Traps fall well within the field of the Deccan Basalts, which suggests that other lateritic horizons in the Kutch and Saurashtra region, developed over Deccan Trap rocks could also have served as sources for the raw material for Ernestites. The mixing model suggests 55-60% contribution from these end-members to the isotopic compositions of most of our samples; however, those from Bhagatrav (in south Gujarat) require ~80% contribution from the sandstones. Therefore, we infer that the Harappans used laterite from different weathered (Deccan) horizons and sand from Mesozoic sandstones from Kutch to manufacture Ernestites.

6. Conclusions

We make the following inferences based on our investigation of Ernestites, the parent material for the unique constricted drill bits of the Harappan Civilization, using petrographic, mineralogical, geochemical, and Sr-Nd isotopic techniques.

1. Stone drill bits have been isotopically fingerprinted to the Ernestites, confirming their genetic link.
2. The Ernestites consist of medium sand to fine silt detrital quartz, hematite, ilmenite, zircon, and rutile welded together in a fine-grained aluminosilicate matrix/groundmass.
3. Ernstite's texture (larger mineral grains and their detrital nature), and its whole-rock Nd isotopic composition ($\varepsilon_{Nd}(0) > -11$) rule out the use of tonstein flint as a raw material.
4. The aluminosilicate matrix/groundmass phase has been chemically identified as pseudomullite, though its XRD spectrum is similar to mullite.
5. The presence of pseudomullites, with high SiO_2 contents (> 40 wt%), unambiguously makes Ernstites artificial, with supporting evidence from the significant substitution of Al_2O_3 and TiO_2 in hematites. These data also suggest a high temperature (reaching 1100 °C) synthesis of Ernestites.
6. Mineralogy, texture, and mineral chemistry suggest Ernstites were manufactured through a high-temperature sintering process involving sand and clay-bearing raw materials.
7. Major and trace element and Sr-Nd isotopic data point to the likelihood of the raw materials' regional provenance (sandstones and laterites of Kutch).
8. All our findings suggest that Ernestites were likely made in the Harappan centers of Gujarat, India, and the Ernestite-based drilling technology was exclusive to this civilization.

Author contributions

JSR and AC conceived the study. AKK, YSR, JSK, and SVR supplied samples. AC, MKM, BGG, NS, and GNSSB conducted the analytical work. MKM, GNSSB, AC, and JSR interpreted the data. JSR secured the project's funding, and all authors contributed to the writing.

Data Availability Statement

All data generated for this study are in the tables in the manuscript and the supplementary files.

Competing interests

The authors declare no competing interests related to this work.

Acknowledgments

JSR thanks the Physical Research Laboratory, Ahmedabad, India, for funding. The authors acknowledge the laboratory support of Sneha Mukherjee of NCESS and Jitender Kumar of PRL.

Appendix A. Supplementary Information

Supplementary materials for this article have been attached as separate files.

1) Supplementary Data 1 (Excel file containing Major and Trace element data for Ernestites)
2) Supplementary Data 2 (Mineral chemistry - EMPA data for various phases in Ernestites)
3) Supplementary Figures (Supplementary Figures 1-6)

References

Banerjee, A., and Chakrabarti, R. (2019). A geochemical and Nd, Sr and stable Ca isotopic study of carbonatites and associated silicate rocks from the~ 65 Ma old Ambadongar carbonatite complex and the Phenai Mata igneous complex, Gujarat, India: Implications for crustal contamination, carbonate recycling, hydrothermal alteration and source-mantle mineralogy.

Baranyai, V. Z., Kristály, F., and Szűcs, I. (2013). Influence of the short time grinding on the thermal decomposition processes of gibbsite produced by the Bayer process. *Materials Science and Engineering*, *38*(1), 15–27.

Bhan, K. K. (2018). Some important aspects of technology and craft production in the Indus civilization with specific reference to Gujarat. *Walking with the unicorn social organization and material culture in ancient south Asia: Jonathan Mark Kenoyer Felicitation Volume*, 48-67.

Bisht, R. S. (2015). *Excavations at Dholavira (1989-90 to 2004-05). A Report Submitted to Archaeological Survey of India. New Delhi.*

Chase, B. P., Ajithprasad, P., Rajesh, S.V., Patel, A., Sharma, B. (2014) Materializing Harappan identities: Unity and diversity in the borderlands of the Indus Civilization. Journal of Anthropological Archaeology, 35, 63-78, ISSN 0278-4165, https://doi.org/10.1016/j.jaa.2014.04.005.

Chandra, J., Paul, D., Stracke, A., Chabaux, F., and Granet, M. (2019). The origin of carbonatites from Amba Dongar within the Deccan large igneous province. *Journal of Petrology*, *60*(6), 1119-1134.

Chatterjee, A. (2018). *Provenance of Late Quaternary Continental Sediments in Western India: Insights from Trace Element and Isotope Geochemistry*. Maharaja Sayajirao University of Baroda (India).

Chatterjee, A., and Ray, J.S. (2017). Sources and depositional pathways of mid-Holocene sediments in the Great Rann of Kachchh, India: Implications for fluvial scenario during the Harappan Culture. *Quaternary International*, *443*, 177–187.

Chatterjee, A., and Ray, J. S. (2018). Geochemistry of Harappan potteries from Kalibangan and sediments in the Ghaggar River: Clues for a dying river. *Geoscience Frontiers*, *9*(4), 1203-1211.

Chatterjee, N. B., and Panti, B. N. (1965). Mullite Refractories from Clay-Bauxite or Quartz-Bauxite Mixes. *Transactions of the Indian Ceramic Society*, *24*(1), 116–121.

Chaudhuri, A., Chatterjee, A., Banerjee, S., and Ray, J. S. (2021). Tracing multiple sources of sediments using trace element and Nd isotope geochemistry: provenance of the Mesozoic succession in the Kutch Basin, western India. *Geological Magazine*, *158*(2), 359–374.

Chaudhuri, A., Schönig, J., Le Pera, E., von Eynatten, H., Chauhan, G., and Lünsdorf, N. K. (2023). Provenance changes revealed by a multi-proxy approach to sandstone analysis and its implications on palaeogeography: Mesozoic Kutch Basin, India. *Sedimentary Geology, 452, 106411.*

Chin, C. L., Ahmad, Z. A., and Sow, S. S. (2017). Relationship between the thermal behaviour of the clays and their mineralogical and chemical composition: Example of Ipoh, Kuala Rompin and Mersing (Malaysia). *Applied Clay Science*, *143*, 327–335.

Cucciniello, C., Demonterova, E. I., Sheth, H., Pande, K., and Vijayan, A. (2015). 40 Ar/39 Ar geochronology and geochemistry of the Central Saurashtra mafic dyke swarm: insights into magmatic evolution, magma transport, and dyke-flow relationships in the northwestern Deccan Traps. *Bulletin of Volcanology*, *77*, 1-19.

Cucciniello, C., Sheth, H., Duraiswami, R. A., Wegner, W., Koeberl, C., Das, T., and Ghule, V. (2020). The Southeastern Saurashtra dyke swarm, Deccan Traps: magmatic evolution of a tholeiitic basalt–basaltic andesite–andesite–rhyolite suite. *Lithos*, *376*, 105759.

Dalim K. Paul, Arijit Ray, Brindaban Das, Shiva K. Patil, Sanjib K. Biswas, Petrology, geochemistry and paleomagnetism of the earliest magmatic rocks of Deccan Volcanic Province, Kutch, Northwest India, Lithos, 102(1–2), 2008, 237-259. https://doi.org/10.1016/j.lithos.2007.08.005.

Deer, W. A., Howie, R. A., and Zussman, J. (2013). *An introduction to the rock-forming minerals*. Mineralogical Society of Great Britain and Ireland.

Dev, J. A., Tomson, J. K., Sorcar, N., and Francis, K. A. (2022). Timing of UHT metamorphism and cooling in south Indian granulites: New PTt results from a sapphirine granulite. *Precambrian Research*, *371*, 106582.

George, B. G., and Ray, J. S. (2017). Provenance of sediments in the Marwar Supergroup, Rajasthan, India: Implications for basin evolution and Neoproterozoic global events. *Journal of Asian Earth Sciences*, *147*, 254–270. https://doi.org/https://doi.org/10.1016/j.jseaes.2017.07.027

Jadhav, G. N., Sharma, N., and Sen, P. (2012). Characterization of bauxite deposits from Kachchh area, Gujarat. *Journal of the Geological Society of India*, *80*, 351-362.

Kanungo A.K. 2021. Harappan Horn Deity Tradition: A Recent Finds at Bhagatrav, *Bulletin of the Deccan College Post-Graduate & Research Institute* 81: 1-16.

Kanungo, A.K., Kaushal R., Bhushan R., Chauhan N., Kharakwal J.S. and Ansari S. 2025. Luminescence and Radiocarbon Chronology of Bhagatrav: A Sorath Harappan Camp Site in South Gujarat, *Radiocarbon* 67(1): 53-73. https://doi.org/10.1017/RDC.2024.119

Kenoyer, J. M. (1997). Trade and technology of the Indus Valley: New insights from Harappa, Pakistan. *World Archaeology*, *29*(2), 262–280. https://doi.org/10.1080/00438243.1997.9980377

Kenoyer, J. M. (2003). Stone Beads and Pendant Making Techniques. In J. W. Lankton (Ed.), *A Bead Timeline: Vol. 1 Prehistory to 1200 CE* (pp. 14–19). Washington DC: The Bead Museum.

Kenoyer, J. M. (2005). Bead technologies at Harappa, 3300- 1900 bc: A comparison of tools, techniques and Finished Beads from the Ravi to the Late Harappan Period,. In C. Jarrige and V. Lefèvre (Eds.), *South Asian Archaeology 2001* (pp. 157–170). CNRS.

Kenoyer, J. M. (2007). Stone beads in Ancient South Asia-7000-600 BC: A comparative approach to technology, style, and ideology. *The Global Perspective of Beads and Beadwork: History, Manufacture, Trade, and Adornment*, 1–12.

Kenoyer, J. M. (2015). The Indus civilization (2600-1900 BC): Early urbanism in South Asia and Its Legacy. *Bulletin of the Shanghai Archaeology Forum 1*, 304–322.

Kenoyer, J. M. (2017a). History of stone beads and drilling: South Asia. *Stone Beads of South and Southeast Asia: Archaeological, Ethnographic and Global Connections*, 127–150.

Kenoyer, J. M. (2017b). History of stone beads and drilling: South Asia. *Stone Beads of South and Southeast Asia: Archaeological, Ethnographic and Global Connections*, 127–150.

Kenoyer, J. M., Cameron, A., Bukhchuluun, D., Amartuvshin, C., Byambatseren, B., Honeychurch, W., Dussubieux, L., and Law, R. (2022). Carnelian beads in Mongolia: new perspectives on technology and trade. *Archaeological and Anthropological Sciences*, *14*(1), 6.

Kenoyer, J. M., and Vidale, M. (1992). A new look at stone drills of the Indus Valley Tradition. *MRS Online Proceedings Library (OPL)*, *267*, 495.

Kharakwal, J. S., Rawat, Y. S., and Osada, T. (2012). Excavations at Kanmer. *Research Institute for Humanity and Nature: Kyoto, Japan.*

Kharakwal, J. S., Rawat, Y. S., Osada, T., & Uesugi, A. (2008). Preliminary observations on the excavation at Kanmer, Kachchh, India 2006–2007. *Linguistics, Archaeology and the Human Past*, 5-23.

Kloprogge, J. T., Ruan, H. D., and Frost, R. L. (2002). Thermal decomposition of bauxite minerals: Infrared emission spectroscopy of gibbsite, boehmite and diaspore. *Journal of Materials Science*, *37*(6), 1121–1129. https://doi.org/10.1023/A:1014303119055/METRICS

Komarneni, S., Schneider, H., and Okada, K. (2005). Mullite synthesis and processing. *Mullite*, 251–348.

Kumar, G. R., and Sreejith, C. (2016). Petrology and geochemistry of charnockites (felsic ortho-granulites) from the Kerala Khondalite Belt, Southern India: Evidence for intra-crustal melting, magmatic differentiation and episodic crustal growth. *Lithos*, *262*, 334-354.

Law, R. W. (2011). *Inter-regional interaction and urbanism in the ancient Indus Valley. A Geological Provenience Study of Harappa's Rock and Mineral Assemblage*. Manohar.

Law, R. W. (2013). The important stone and metal resources of Gujarat during the Harappan period. *Heritage: Journal of Multidisciplinary Studies in Archaeology*, *1*, 319–343.

Lenz, S., Birkenstock, J., Fischer, L. A., Schüller, W., Schneider, H., and Fischer, R. X. (2019). Natural mullites: chemical composition, crystal structure, and optical properties. *European Journal of Mineralogy*, *31*(2), 353–367.

Locsei, B. P. (1968). Possible technical developments in the manufacture of fireclay refractory materials: III, Mechanisms of the synthesis of mullite in the system kaolinite-aluminum fluoride. *Keram. Z*, *20*, 362–367.

Ludvik, G. E., Kenoyer, J. M., Klonymus, H. C., Barkay, G., and Dvira, Z. (2022). Stone beads from the temple mount, Jerusalem: a relative chronology through high-resolution studies of bead technology. *Archaeological and Anthropological Sciences*, *14*(6), 115.

Mackay, E. J.H. (1937). Bead making in ancient Sind. *Journal of the American Oriental Society*, *57(1), 1-15.*

Mackay, E. J. H. (1938). Further Excavations at Mahenjo-daro. Government of India, New Delhi.

561 Mandal, A., Koner, A., Sarkar, S., Tawfik, H. A., Chakraborty, N., Bhakta, S., and Bose, P. K.
562 (2016). Physico-chemical tuning of palaeogeographic shifts: Bhuj formation, Kutch, India.
563 *Marine and Petroleum Geology*, *78*, 474–492.

564 McCarthy, B., Vandiver, P. Ancient High-Strength Ceramics: Fritted Faience Bracelet
565 Manufacture at Harappa (Pakistan), Ca. 2300-1800 B.C.. *MRS Online Proceedings*
566 *Library* **185**, 495–510 (1990). https://doi.org/10.1557/PROC-185-495

567 McDonough, W. F., and Sun, S. S. (1995). The composition of the Earth. *Chem. Geol*, *120*,
568 223-253.

569 Meshram, R. R., and Randive, K. R. (2011). Geochemical study of laterites of the Jamnagar
570 district, Gujarat, India: Implications on parent rock, mineralogy and tectonics. *Journal of*
571 *Asian Earth Sciences*, *42*(6), 1271–1287.

572 Moecher, D. P., and Brearley, A. J. (2004). Mineralogy and petrology of a mullite-bearing
573 pseudotachylyte: Constraints on the temperature of coseismic frictional fusion. *American*
574 *Mineralogist*, *89*(10), 1486–1495.

575 Nath J. and Kumaran R.N. (2017). Khirsara-A Harappan Metropolis in Western Kachchh,
576 Gujarat, India, *Heritage: Journal of Multidisciplinary Studies in Archaeology* 5: 541-555.

577 Navias, L., and Davey, W. P. (1925). Differentiation between mullite and sillimanite by their
578 X-ray diffraction patterns 1. *Journal of the American Ceramic Society*, *8*(10), 640–647.

579 Noghani, S., & Emami, M. (2014). Mineralogical phase transition on sandwich-like structure
580 of clinky pottery from parthian period, Iran. *Periodico di Mineralogia*, *83*(2).

581 Periasamy, V., and Venkateshwarlu, M. (2017). Petrography and geochemistry of Jurassic
582 sandstones from the Jhuran Formation of Jara dome, Kachchh basin, India: Implications for
583 provenance and tectonic setting. *Journal of Earth System Science*, *126*, 1–20.

584 Pokharia A.K., Agnihotri R., Sharma S., Bajpai S., Nath J., Kumaran R.N. and Negi B.C.
585 (2017) Altered cropping pattern and cultural continuation with declined prosperity following
586 abrupt and extreme arid event at ~4,200 yrs BP: Evidence from an Indus archaeological site
587 Khirsara, Gujarat, western India. *PLoSONE* 12(10): e0185684.
588 https://doi.org/10.1371/journal.pone.0185684

589 Potts P.J. and Kane J.S. (2003) International Association of Geoanalysts Certificate of
590 Analysis: Certified Reference Material OU-6 (Penrhy Slate). *Geostandards and*
591 *Geoanalytical Research*, 29, 233-236.

592 Prabhakar, V. N. (2016). An overview of the stone bead drilling technology in South Asia
593 from earliest times to Harappans. *Heritage: Journal of Multi-Disciplinary Studies in*
594 *Archaeology*, *4*, 47–74.

595 Prabhakar, V. N., Bisht, R. S., Law, R. W., and Kenoyer, J. M. (2012). Stone Drill Bits from
596 Dholavira: A multifaceted analysis. *Man and Environment*, *37*(1), 8–25.

597 Pracchia, S., Vidale, M., & Volpicelli, O. (1993). The Archaeological Context of Stoneware
598 Firing at Mohenjo-Daro. *East and West*, *43*(1/4), 23–68. http://www.jstor.org/stable/29757083

599 Prasad, R. K., and Prabhakar, V. N. (2022). Mineralogical characterization of raw materials
600 from Dholavira, Gujarat, India and its geological and archaeological significance. *Current*
601 *Science (00113891)*, *123*(11).

Querol, X., Fernandez Turiel, J. L., & Lopez Soler, A. (1994). The behaviour of mineral matter during combustion of Spanish subbituminous and brown coals. *Mineralogical Magazine*, *58*(390), 119–133. doi:10.1180/minmag.1994.058.390.11

Rossini, A. R., Arazi, S. C., and Krenkel, T. G. (1970). Mullitization of mixtures of kaolinitic clay and aluminium hydroxides. *Bol. Soc. Espan. Ceram*, *9*, 579–591.

Barthelmyde Saizieu, B. and Bouquillon, A. (1994) Steatite working at Mehrgarh during the Neolithic and Chalcolithic periods: quantitative distribution, characterization of material and manufacturing processes. Pp. 47-59 in A. Parpola and P. Koskikallio (eds), South Asian Archaeology 1993, Volume I. Proceedings of the Twelfth International Conference of the European Association of South Asian Archaeologists, Helsinki University 5-9 July 1993. Helsinki: Suomalainen Tiedeakatemia.

Schneider, H., Schreuer, J., and Hildmann, B. (2008). Structure and properties of mullite—a review. *Journal of the European Ceramic Society*, *28*(2), 329–344.

Septawendar, R. (2007). Sifat fisik lempung Tanjung Morawa dalam transformasi fasa mineral berdasarkan investigasi difraksi Sinar X. *Riset Geologi Dan Pertambangan*, *17*(1), 11–19.

Shears, E. C., and Archibald, W. A. (1954). Aluminosilicate refractories. *Iron Steel*, *27*, 26–30.

Sheth, H. C., Ray, J. S., Ray, R., Vanderkluysen, L., Mahoney, J. J., Kumar, A., ... and Jana, B. (2009). Geology and geochemistry of Pachmarhi dykes and sills, Satpura Gondwana Basin, central India: problems of dyke-sill-flow correlations in the Deccan Traps. *Contributions to Mineralogy and Petrology*, *158*, 357-380.

Simonetti, A., Goldstein, S. L., Schmidberger, S. S., and Viladkar, S. G. (1998). Geochemical and Nd, Pb, and Sr isotope data from Deccan alkaline complexes—inferences for mantle sources and plume–lithosphere interaction. *Journal of Petrology*, *39*(11-12), 1847-1864.

Singh, B. P., and Srivastava, V. K. (2019). Petrographical, mineralogical, and geochemical characteristics of the Palaeocene lateritic bauxite deposits of Kachchh Basin, Western India. *Geological Journal*, *54*(4), 2588–2607.

Sun, S. S., and McDonough, W. F. (1989). Chemical and isotopic systematics of oceanic basalts: implications for mantle composition and processes. *Geological Society, London, Special Publications*, *42*(1), 313-345.

Sorcar, N., Mukherjee, S., Pant, N. C., Dev, J. A., and Nishanth, N. (2021). Chemical dating of monazite: Testing of analytical protocol for U–Th–total Pb using CAMECA SXFive tactis EPMA at the National Centre for Earth Science Studies, Thiruvananthapuram, India. *Journal of Earth System Science*, *130*, 1–11.

Thirlwall, M. F. (1991). Long-term reproducibility of multicollector Sr and Nd isotope ratio analysis. *Chemical Geology: Isotope Geoscience Section*, *94*(2), 85–104.

Tripati, S., Ray, J. S., Behera, R. P., Babu, P., Mahala, M. K., Kocherla, M., and Khedekar, V. (2022). Geochemical provenance of an Indo-Arabian stone anchor from Manikapatna highlights the medieval maritime trade of India. *Scientific Reports*, *12*(1), 13559.

Vidale, M. (2000). The archaeology of Indus crafts: Indus craftspeople and why we study them. Istituto Italiano per l"Africa el'Oriente, Rome.

644 Worral, W. E. (1968). *Clays: their nature, origin and general properties*. Elsevier Science
645 Ltd.

646 Wentworth, C.K. (1922). A scale of grade and class terms for clastic sediments. The Journal
647 of Geology, 30(5), 337-424. https://doi.org/10.1086/622910

648 Yanti, E. D., and Pratiwi, I. (2018). Correlation between thermal behavior of clays and their
649 chemical and mineralogical composition: A review. *IOP Conference Series: Earth and*
650 *Environmental Science*, *118*(1), 12078.

651

652 **Figures**

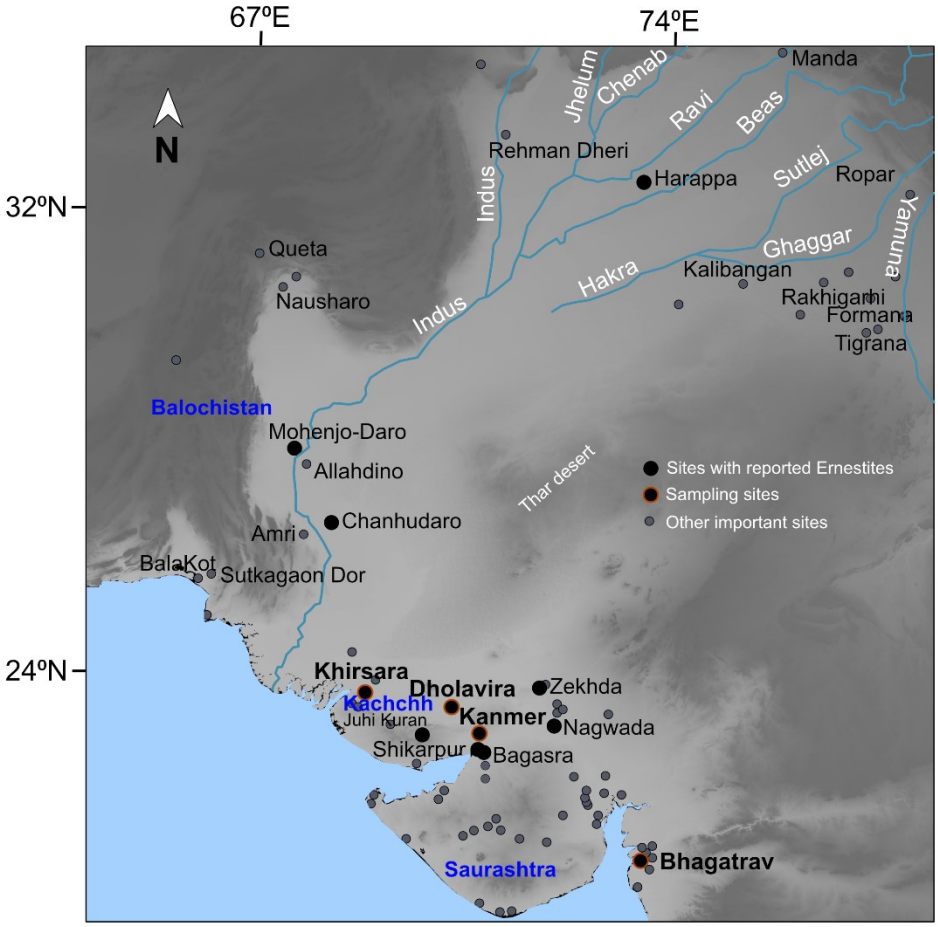

653

654 **Figure 1**. A schematic geographical map of western India and Pakistan shows important
655 Harappan urban centers and cities yielding Ernestite stones and drill bits. The four Harappan
656 sites whose Ernestite samples have been studied in this work are marked.

657

658

659 **Figure 2**. (a) Ernestite stones from Dholavira, Bhagatrav, and Kanmer studied in this work.
660 Note the compositional variations between different samples, as reflected in their colors. (b)
661 Ernestite drill bits from Kanmer. Note the compositional variations. The first and third
662 samples have been used for isotopic analyses.

663

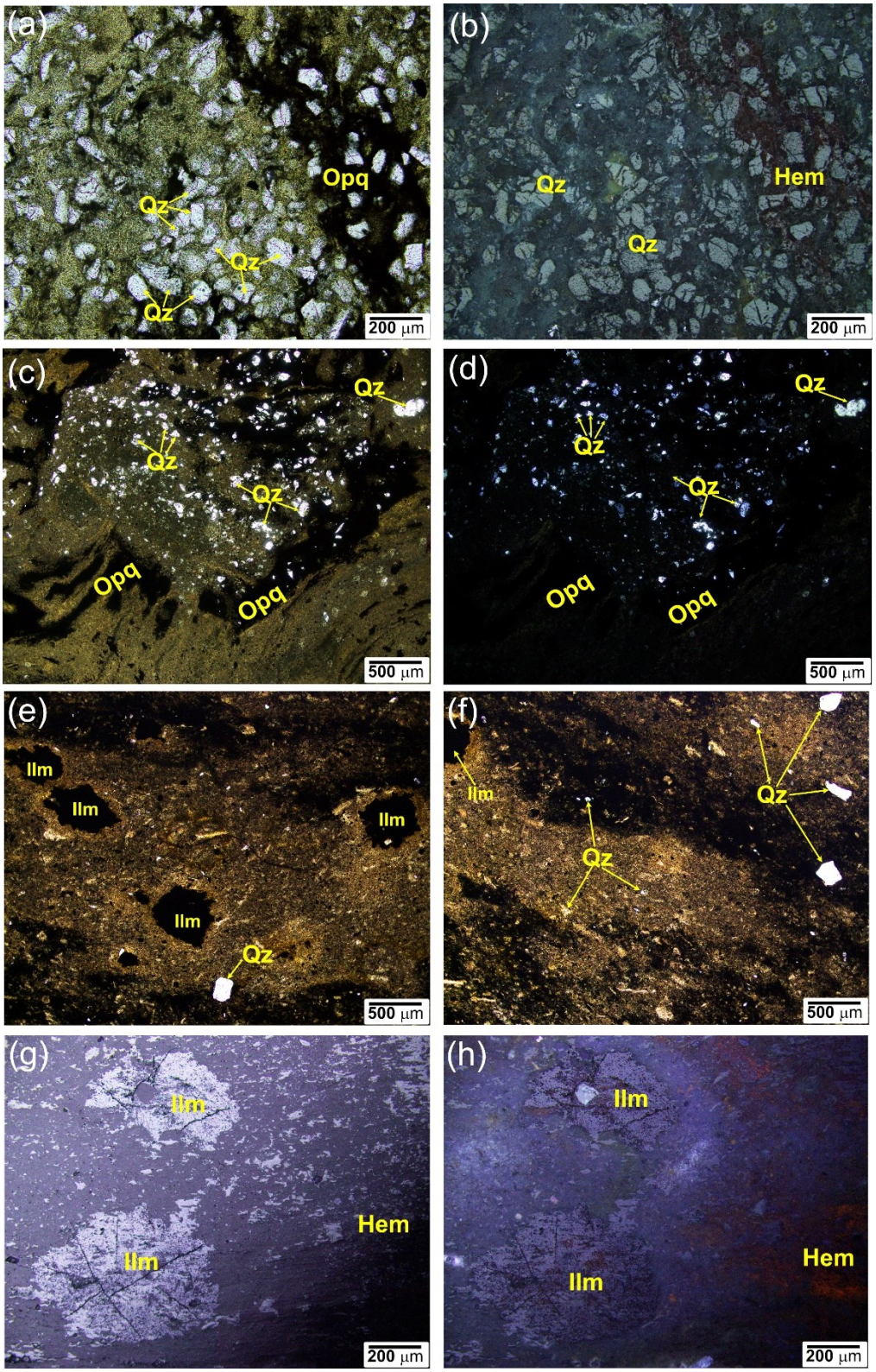

Figure 3. Photomicrographs of Ernestite thin sections: (a) sample from Dholavira in plane-polarized transmitted light showing the presence of quartz (Qz) and opaques (Opq); (b) same as in (a) with hematite (Hem) displaying characteristic red internal reflection under reflected lights; (c-d) sample from Bhagatrav in plane-polarized and cross-polarized transmitted lights; (e-f) sample from Kanmer showing detrital ilmenite (Ilm) and quartz (Qz) in plane-polarized transmitted light; (g-h) sand-sized ilmenite (Ilm) grains and hematite (Hem) patches in the same sample as in (e) in plane and crossed polarized reflected lights, respectively.

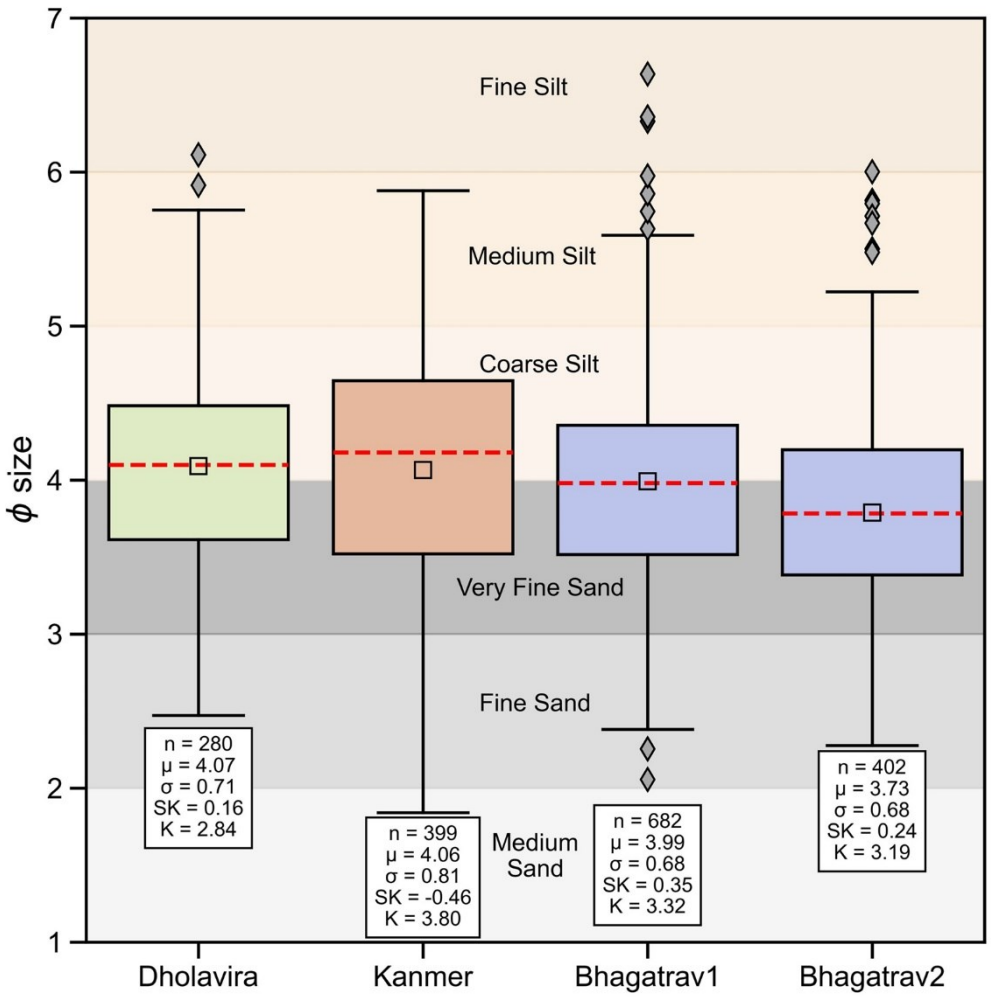

672

673 **Figure 4**. Boxplot showing grain size distribution (in ϕ scale) in the Ernestites. Relevant
674 statistical information is given in boxes inside the figure. The mean (square) and median (red
675 dashed line) are marked in each box. Bhagatrav-1 and Bhagatrav-2 represent the yellow
676 (khaki) and black colored groundmasses, respectively. Symbols: n= number of observations;
677 μ = mean; σ = standard deviation; SK = skewness; K = Kurtosis.

678

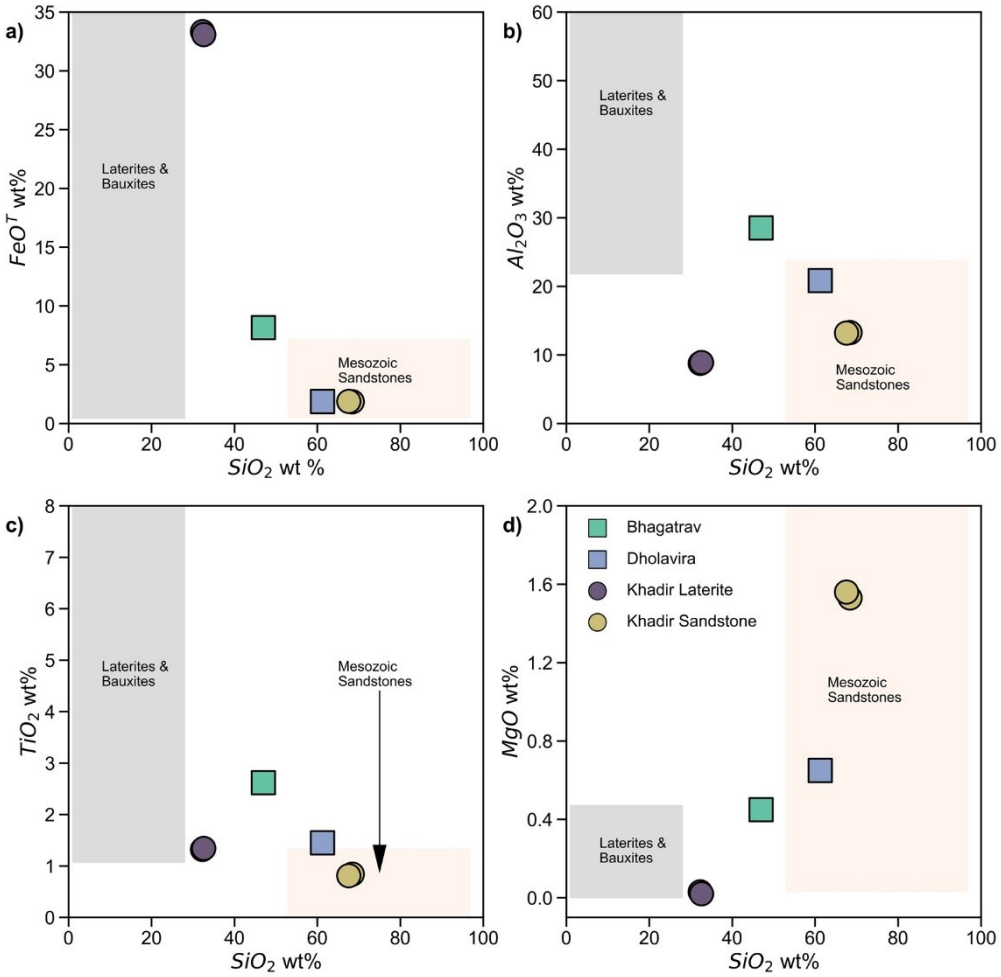

679

680 **Figure 5**. Plots of various oxides vs SiO_2 for Ernestites of Gujarat, laterites, and sandstones
681 from Khadir Island (data in Table 1). Compositions of Mesozoic sandstones and laterites and
682 bauxites of Kutch are plotted as fields for comparison. Data sources for the latter: Mandal et
683 al. (2016); Periasamy and Venkateshwarlu (2017); Jadhav et al. (2012); Meshram and
684 Randive (2011); Singh and Srivastava (2018).

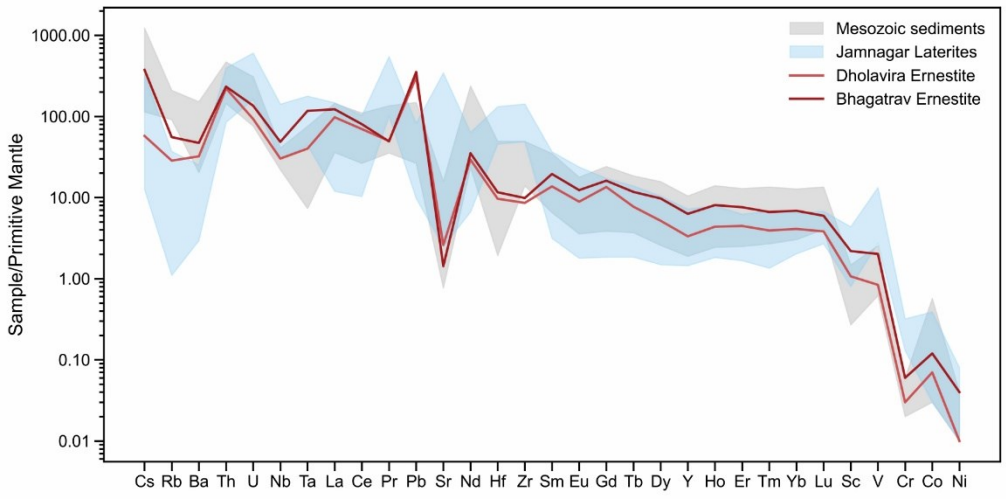

685

686 **Figure 6**. Primitive Mantle normalized spider diagram for Ernestites of Gujarat. Also plotted
687 are the data for Mesozoic shales and laterites of Kutch (Data sources: Chaudhury et al., 2020;
688 Meshram and Randive, 2011). Normalizing values are from Sun and McDonough (1989) and
689 McDonough and Sun (1995).

690

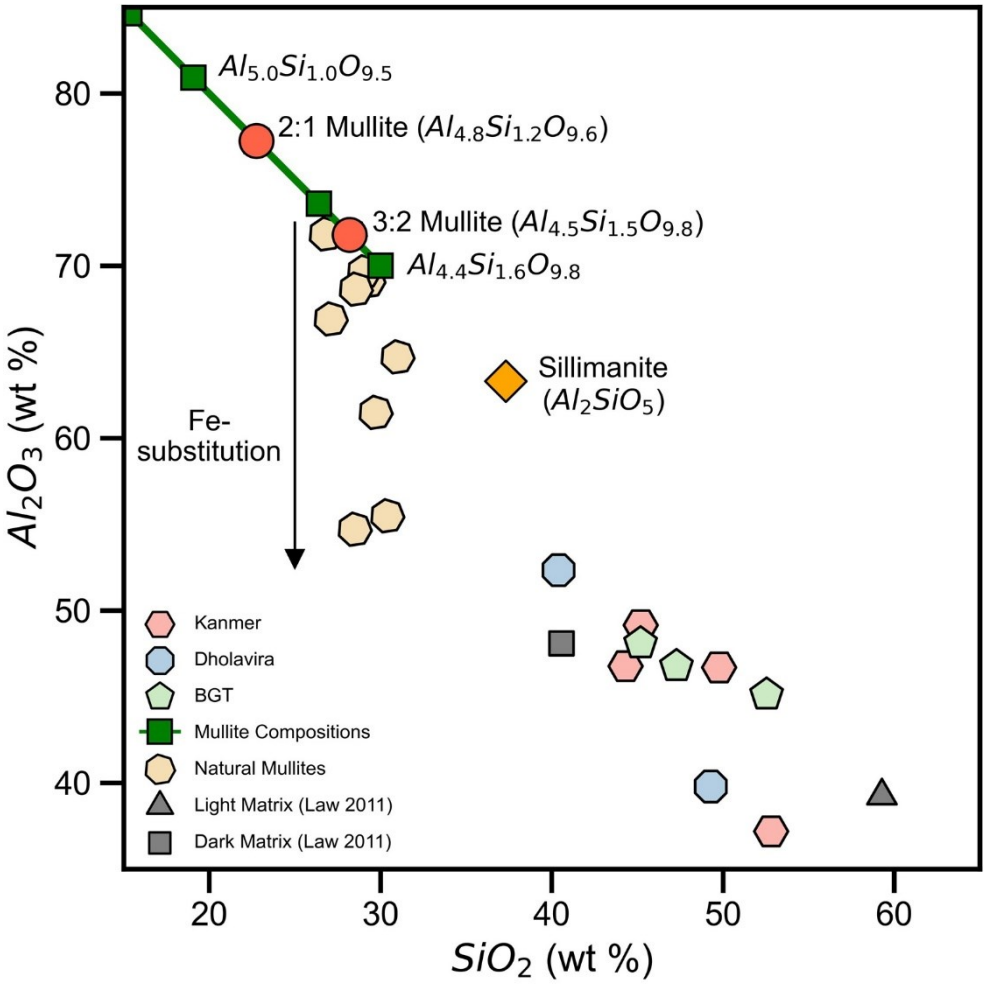

691

692 **Figure 7**. The plot of Al_2O_3 vs. SiO_2 for the aluminosilicate phases in our Ernestite samples
693 compared with compositions of natural mullite, stoichiometric (synthetic) mullite, mullite
694 solid solution, and stoichiometric sillimanite. Data sources: Natural mullite - Moecher and
695 Brearley (2004); Lenz et al. (2019).

696

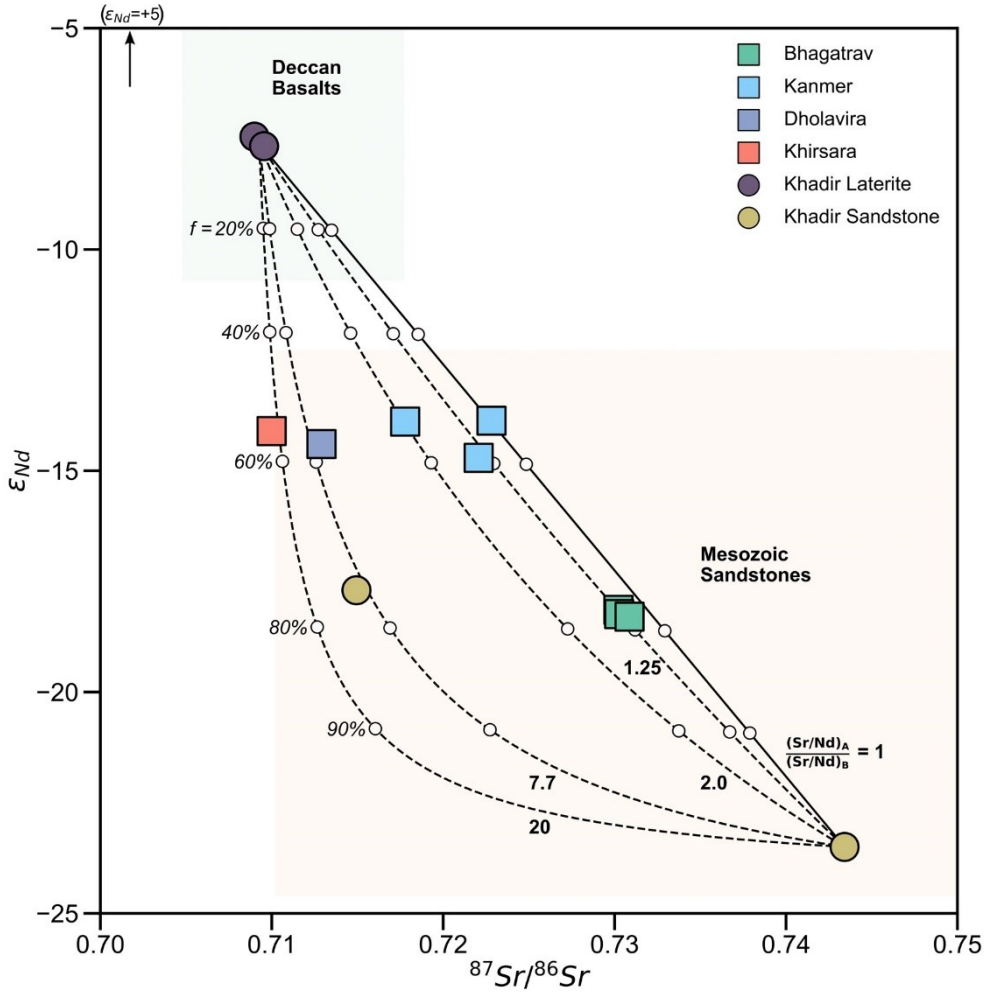

Figure 8. The plot of $\varepsilon_{Nd}(0)$ vs. $^{87}Sr/^{86}Sr$ of the Ernestite stones and drill bits, along with laterites and sandstones from Khadir Island. The compositional fields for Deccan Basalts and Mesozoic sedimentary rocks (sandstones) of Kutch are also shown for comparison. The curves represent binary mixing curves between a sandstone ($^{87}Sr/^{86}Sr$ = 0.743415; ε_{Nd} = -23.5) and a laterite ($^{87}Sr/^{86}Sr$ = 0.70927; ε_{Nd} = -7.6). The sandstone end-member (A) composition is similar to a Mesozoic sandstone of Kutch, and the laterite (B) is from Khadir (Table 4); *f* represents the fraction of sand end-member in the mixture. Data sources: Deccan Basalts - Simonetti et al. (1998); Paul et al. (2008); Sheth et al. (2009); Cucciniello et al. (2015), (2020); Banerjee and Chakrabarti (2019); Chandra et al. (2019) and Mesozoic sandstones – Chatterjee (2017).